Published online 20 March 2009 *Nucleic Acids Research, 2009, Vol. 37, No. 10* ***3165–3176***
doi:10.1093/nar/gkp165

Lesion-induced DNA weak structural changes detected by pulsed EPR spectroscopy combined with site-directed spin labelling

Giuseppe Sicoli[1], Gérald Mathis[2], Samia Aci-Sèche[3], Christine Saint-Pierre[2], Yves Boulard[3], Didier Gasparutto[2,*] and Serge Gambarelli[1,*]

[1]Laboratoire de Résonance Magnétique, [2]Laboratoire Lésions des Acides Nucléiques, Service de Chimie Inorganique et Biologique UMR-E n°3 CEA-UJF FRE 3200 CNRS/Institut des Nanosciences et Cryogénie, CEA-Grenoble, 17, Avenue des Martyrs, F-38054, Grenoble Cedex 9 and [3]Laboratoire de Biologie Intégrative, Service de Biologie Intégrative et Génétique Moléculaire, Institut de Biologie et de Technologies de Saclay; CEA-Saclay, F-91191, Gif-sur-Yvette Cedex, France

Received 25 November 2008; Revised 5 February 2009; Accepted 1 March 2009

ABSTRACT

Double electron-electron resonance (DEER) was applied to determine nanometre spin–spin distances on DNA duplexes that contain selected structural alterations. The present approach to evaluate the structural features of DNA damages is thus related to the interspin distance changes, as well as to the flexibility of the overall structure deduced from the distance distribution. A set of site-directed nitroxide-labelled double-stranded DNA fragments containing defined lesions, namely an 8-oxoguanine, an abasic site or abasic site analogues, a nick, a gap and a bulge structure were prepared and then analysed by the DEER spectroscopic technique. New insights into the application of 4-pulse DEER sequence are also provided, in particular with respect to the spin probes' positions and the rigidity of selected systems. The lesion-induced conformational changes observed, which were supported by molecular dynamics studies, confirm the results obtained by other, more conventional, spectroscopic techniques. Thus, the experimental approaches described herein provide an efficient method for probing lesion-induced structural changes of nucleic acids.

INTRODUCTION

The constant assault on cellular constituents by endogenous and exogenous agents leads to a large set of DNA alterations. DNA strand breaks, abasic sites, oxidized bases, oxidatively fragmented products, base deamination products, nucleotide alkylation products, pyrimidine photoproducts and cross-linked bases are some examples of the most common DNA damages identified at the cellular level (1–3). Such lesions are often related to conformational changes and relative movements of domains on the nanometre scale that may have a high biological impact in terms of lethality and mutagenicity. Thus, various DNA repair, DNA replication and DNA transcription processes are strongly affected by the presence of alterations in the biopolymer, with consequences directly linked to the complexity and the diversity of the modified chemical structures involved (4–6). The analyses of lesion-induced structural changes, which can be accessed by distance measurements, may provide new insights allowing a better elucidation of the structure-toxicity relationship (7–10). Up to now, distance determinations related to DNA structure changes induced by lesions, have mainly been determined by X-ray crystallography, high-resolution NMR spectroscopy (11) and, in selected cases, by fluorescence resonance energy transfer (FRET) (12,13). However, although such techniques can provide exhaustive information on the characterization of DNA structures, they still exhibit some drawbacks: NMR is restricted to a limited size of molecule and can provide only short-range direct distance determinations; X-ray crystallography is dependent on the availability of a crystal structure; FRET spectroscopy can measure a very long-range distance, but it provides an average information if several different conformers are present (14); similar limitations, especially for the analysis of

*To whom the correspondence should be addressed. Tel: +33-4-38-78-39-40; Fax: +33-4-38-78-50-90; Email: serge.gambarelli@cea.fr
Correspondence may also be addressed to Didier Gasparutto. Tel: +33-4-38-78-45-58; Fax: +33-4-38-78-50-90; Email: didier.gasparutto@cea.fr

The authors wish it to be known that, in their opinion, the first two authors should be regarded as joint First Authors.

oligonucleotide structures, are faced when using circular dichroism (15–17).

Recently, site-directed spin labelling (SDSL) combined with pulsed EPR techniques (DEER and Double Quantum Coherence) (18,19) have been applied to several large biomacromolecules in order to measure long-range interspin distances between nitroxide spin labels and to characterize overall structures with intrinsic flexibility (i.e. when more than one stable conformation can be observed). Over the past few years, these methods led to the determination of the structure of soluble proteins (20), peptides (21), membrane proteins (22), RNA and DNA (23–25). Following a successful detailed detection of *B*/*A* conformational transitions of double-stranded DNA (dsDNA) and DNA–RNA duplexes by DEER experiment (26), we wished to attempt the detection of damage-induced DNA conformational changes by using this spectroscopic technique. For this purpose, distance measurements on selected undamaged and damaged SDSL-duplexes that contain an 8-oxoguanine (8-oxoG), a nick, a gap, a bulge, an abasic site analogue (namely tetrahydrofuran, THF) or anucleosidic sites (ethyl and propyl residues), were performed and the findings were supported by molecular dynamics studies. This provides an accurate elucidation of the overall structure of the modified nucleic acid fragments, as well as further information concerning the flexibility of the biomolecule. A detailed description of the lesion-induced DNA structures may provide new insights into how DNA–protein complexes are formed, and into selective repair mechanisms and mutagenic processes.

MATERIALS AND METHODS

Reagents and general methods

All reagents were purchased from Sigma-Aldrich (Saint Quentin-Fallavier, France). UV absorbance spectra were measured on an Uvikon 930 spectrophotometer. MALDI-ToF mass spectrometry measurements were performed with a Biflex spectrometer (Bruker), using 3-hydroxypicolinic acid as a matrix and ammonium citrate as a cation exchanger, as previously described (27).

Synthesis, purification and characterization of oligonucleotides

All the oligonucleotides (Figures 1 and 2) were prepared by solid-phase syntheses on an Applied Biosystems 392 DNA/RNA synthesizer using phosphoramidite chemistry on a scale of 1 μmol. Phenoxyacetyl (Pac) group was used to protect the amino function of 2′-deoxyguanosine and 2′-deoxyadenosine, and the acetyl (Ac) group for 2′-deoxycytidine. The solid support was a succinyl long-chain alkylamine controlled-pore-glass (Succ-LCCA-CPG). Stepwise coupling efficiencies were measured automatically on the synthesizer by dimethoxytrityl analysis.

DNA fragments containing nitroxide spin labels (one or two TEMPO probes) were synthesized according to the previously described protocol (26,28). Briefly, internal site-specific labelling was performed by on-support post-synthetic insertion of the TEMPO unit into a 2-fluorohypoxanthine, initially incorporated into the oligonucleotide sequence by using a commercially available 2-fluoro-Inosine phosphoramidite monomer (Glenresearch, VA, USA). This site-specific substitution was performed by incubating the protected DNA fragments containing two 2-fluorohypoxanthine bases, attached to the solid support, with a concentrated amino-TEMPO solution (1 M in DMSO) overnight at 50°C. Deprotection and cleavage from the support were performed first by a 1 M DBU solution in anhydrous methanol, at room temperature for 2 h (2 × 1 h), followed by treatment with aqueous ammonia (NH_4OH 30%) for 16 h at 55°C. Finally, double nitroxide-labelled DNA fragments were purified by reversed-phase HPLC. Experimental yield was approximately 30%.

Oligonucleotides containing the 8-oxo-7,8-dihydro-2′-deoxyguanosine were obtained following the previously described methods (29). Sequences containing an abasic site analogue, tetrahydrofuran (THF), and anucleosidic sites, ethyl- and propyl-spacer, were prepared using commercially available monomers according to the manufacturer's protocol (Glenresearch, VA, USA) in the trityl-on mode. Upon completion, the latter oligonucleotides were deprotected in concentrated aqueous ammonia for 16 h at 55°C. After speed-vac evaporation of ammonia, the crude 5′-DMTr oligonucleotides were detritylated and purified on-line by reversed phase-HPLC using a polymeric support (30).

After desalting by size exclusion on Pharmacia NAP-25 columns, all the purified oligonucleotides were then quantified by UV absorption at 260 nm. Finally, the purity and the integrity of the synthetic DNA fragments were verified by RP-HPLC analyses together with MALDI-ToF mass measurements (data not shown). Samples were then lyophilized and frozen at –20°C until use.

Preparation of the lesion- and nitroxide-containing double-stranded DNA constructs

Single-stranded DNA (ssDNA, 3 or 6 nmoles, for a final concentration of 50 or 100 μM, respectively) labelled with the nitroxide spin probes was mixed with a complementary sequence (1.5 eq.) (undamaged ssDNA or containing a selected lesion) at room temperature in a 60 μl final volume of binding buffer containing 25 mM Tris–HCl (pH 7.4), 0.1 M NaCl, 1 mM EDTA Na_2 in deionized water (60 μl final vol.). This mixture was then heated to 90°C for 3 min and slowly cooled to 25°C to allow hybridization.

Before insertion into the resonator, 15–20% glycerol as a cryoprotectant was added to the sample, followed by flash freezing using liquid nitrogen. After preliminary spectroscopic analysis, a further 0.5 eq. of the complementary sequence was added; the heating-cooling steps were repeated, followed by freezing of the sample and the DEER experiment. This procedure has been repeated until no changes into the dipolar evolution and distance distribution could be observed due to the addition of further complementary sequence.

DEER experiments (standard set up)

DEER measurements were performed using a Bruker EleXsys 580 spectrometer equipped with a 5 mm dielectric ring resonator at the temperatures of 60 or 70 K (related to the [4;19] and [4;11] duplexes, respectively). The four-pulse DEER sequence $(\pi/2)_{\nu 1} - \tau_1 - (\pi)_{\nu 1} - \tau - (\pi)_{\nu 2} - \tau_1 + \tau_2 - \tau - (\pi)_{\nu 1} - \tau_2$–echo was used in each of the DNA distance determinations (Supplementary Data). The ELDOR pulse (ν_2, 32 ns) was positioned at the centerfield maxima of the echo-detected nitroxide spectrum, whereas the $\pi/2$ and π observe pulses (ν_1, 16 and 32 ns) were positioned at the low field line of the spectrum ($\nu_1 - \nu_2 \approx 75$ MHz). A model-free analysis of DEER data was performed by applying Tikhonov regularization, using the L curve as criterion for optimal parameter regularization (31). Primary experimental data were background-corrected by fitting a decay function $B(t)$ for the intermolecular contribution, followed by normalization of the function. The form factor $F(t)$ obtained in this way was then processed by Tikhonov regularization. All model-free processing was performed with the program DeerAnalysis 2006-07 (31). Tikhonov regularization might be affected by low signal/noise (S/N) ratio, short evolution time, and incorrect fitting of the decay. Therefore, for each of these factors we carefully tested different conditions (see 'Results' section).

DEER experiments (orientation averaging)

Compared to the standard set-up of DEER sequence, for the orientation averaging experiment the observer-field value was varied (in the previous case it had a fixed value), adding 10 traces with a B_0 increment of 0.3 mT. All the other parameters were kept unchanged with respect to the values described above.

Molecular dynamics studies

All initial models for the duplexes were built in *B*-form using the Leap module of the AMBER 9.0 package. MD simulations were performed with the AMBER 9.0 program package. Force-field parameters for non-standard residues such as the ^{TEMPO}G residue, the 8-oxoG residue or the THF residue were computed using the Gaussian 03 program and fitted with the RESP program for compatibility with the AMBER99 force field. All systems were minimized and simulated with the same protocol, described in previous work (26), during a production period of 10ns, where the coordinates were saved every picosecond for analysis. Interspin distances were extracted from whole trajectories using the ptraj module of the AMBER 9.0 package. Mean distance is directly extracted from the kinetic distance data for comparison with the experimental. Histograms of distance distributions were constructed with intervals of 0.1 Å using the Xmgrace program and a gaussian fitting was performed on these curves to enable the extraction of the calculated width at half-height.

RESULTS

Synthesis of damaged and spin-labelled DNA duplexes

Figure 1 depicts the different steps required to obtain DNA structural patterns allowing easy insertion (and detection) of selected DNA lesions or modifications. A single-stranded DNA sequence was doubly labelled and hybridization with the lesion-containing complementary strand allowed us to obtain the desired systems. Furthermore, these original constructs allow the evaluation of distance changes as a function of the nature of the defects within the DNA duplex (Figure 2), as well as its position in the biopolymer. A convenient synthetic approach was developed to prepare a set of double spin-labelled and damaged DNA duplexes (Figure 1). First, the nitroxide spin-labels were site-specifically incorporated at position 2 of two guanine bases by an on-support post-synthetic substitution of the fluorine atom of 2-fluorohypoxanthine residues by 2-amino tempo (^{TEMPO}G). This synthetic approach, adapted from an initial work published by Saito and collaborators (28), allows simultaneous introduction of the nitroxide probes at two different positions on the polynucleotide chain (26). The structural impact of several relevant DNA alterations (nick, gap, bulge, modified base) that have been shown to form at the cellular level was then studied. A nicked structure lacks a phosphate bond between two adjacent bases, while a duplex containing a gap structure is composed by the 20-mer ssDNA containing the two nitroxide spin probes and two complementary ssDNA formed by 7 and 12 bases, respectively (Figure 2). The bulge structure derives from an unpaired base, i.e. an additional adenine base A_1 inserted into the complementary sequence. For the abasic site lesions, several stable analogues were prepared, namely a tetrahydrofuran, a propyl and an ethyl unit (Figure 2), and then used to evaluate the performance of the current spectroscopic method. Preparation of the DNA fragments containing an 8-oxoG residue, a well-known oxidative base lesion, was performed as previously described (29). All the other targeted lesion-containing sequences were generated using commercially available monomers following the supplier's recommendations. After purification by HPLC, the integrity and purity of the modified synthetic oligonucleotides were checked by analytical HPLC and mass spectrometry measurements (data not shown).

DEER analyses on undamaged DNA duplexes

In order to establish a reference distance, the first DEER experiments were carried out on undamaged DNA duplexes, where two nitroxide spin probes were introduced on a single-stranded DNA (ssDNA) at positions [4;11] and [4;19], respectively (Figure 2). The addition of the complementary sequence and the corresponding formation of the double-stranded DNA (dsDNA) produced systems which exhibited a remarkably narrow distribution, with main peaks centred at 2.81 nm and 5.21 nm, respectively. The widths for these distance distributions w (width at half height of the distance distribution, 0.21 nm for the [4;11] and 0.33 nm for the [4;19] duplex)

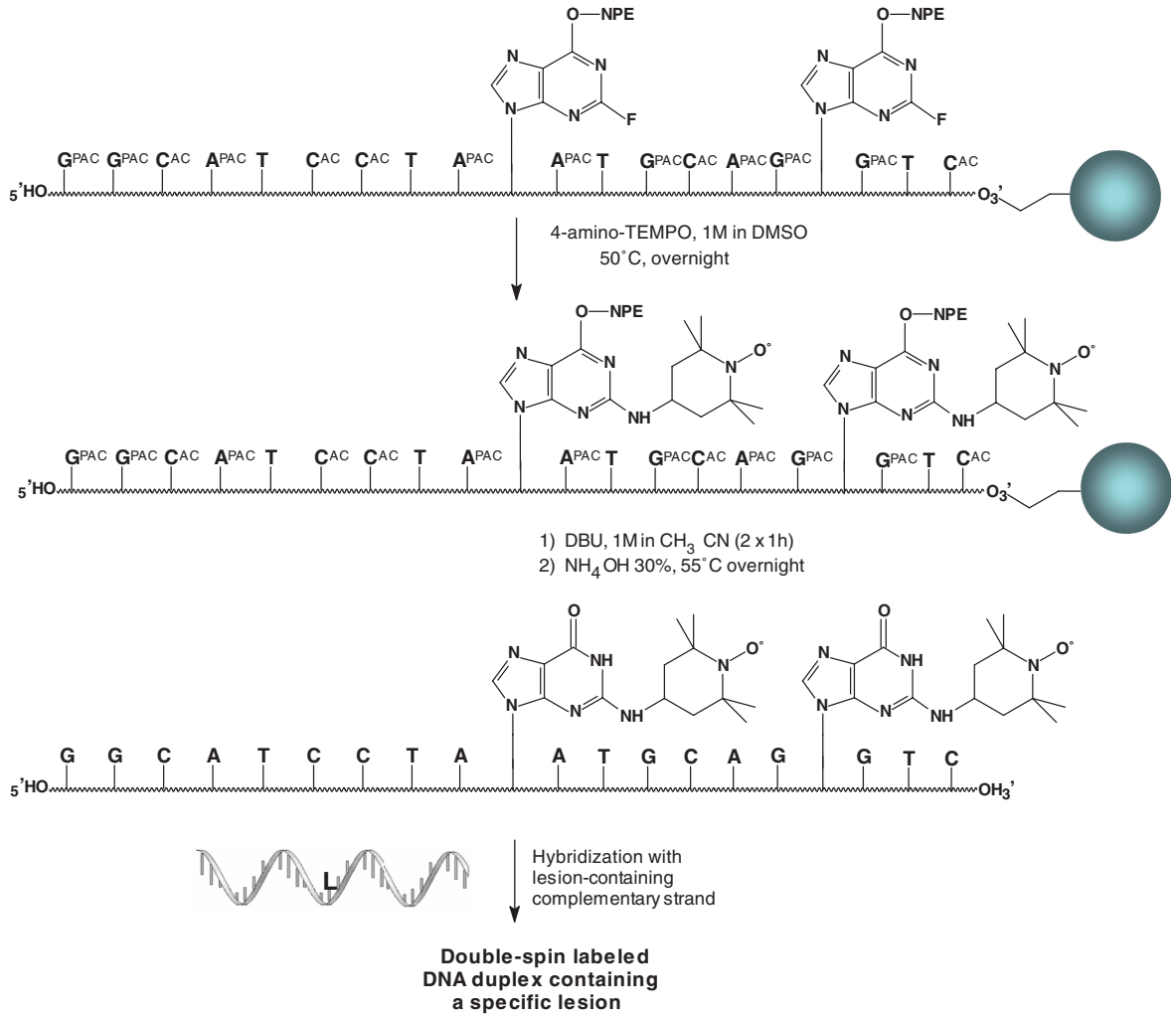

Figure 1. Synthetic route to lesion-containing double-spin labelled DNA probes for pulsed EPR spectroscopy structural analyses.

suggested the presence of a surprisingly rigid structure, compared to analogous labelled systems described in the literature (32–34). This system is therefore ideally suited to the detection of even small conformational changes. The origin of this effect is probably due to the combination of the chemical nature of the spin label and the localization of both labels on one strand (see ref. 26).

Close examination of the distance distribution of duplexes [4;11] and [4;19] reveals a much smaller peak at 2.25 nm and 4.25 nm, respectively. This can be attributed to a deformation of the edges of the Pake pattern (Supplementary Figure S1). This is a well known minor drawback of the standard set-up of the four pulse DEER sequence when applied to rigid systems (35). According to the literature (36,37), an orientation averaging experiment can be carried out to overcome this drawback. This consists of sweeping the magnetic field so that the observer position is between the low-field edge and the central peak of the nitroxide spectrum in several steps (typically 10–20 steps); the sum of the different spectra will *virtually* eliminate orientation selection and systematic deviations of the fit (Figure 3). When applied to the previous systems, this orientation averaging DEER experiment strongly reduces the smaller peaks in the distance distribution (Figure 3) while maintaining the same width w. It must be noted that in both standard and orientation averaging DEER experiments, a slight asymmetry of the distance distribution is observed for the undamaged [4;11] DNA system. This may be an indication of the intrinsic flexibility of the labelled system.

[4;11] Damaged DNA duplexes analysed by DEER

The undamaged systems will be taken as reference dsDNA in order to describe slight or strong distortion induced by DNA lesions (Figure 2). Most of our analysis of DNA damage-induced conformational change were carried out on the [4;11] duplex, due to the possibility to reduce the acquisition time and sample concentration while working on a moderate interspin distance (around 3 nm) (7). Selected analyses on the [4;19] duplex confirmed observations. Screening the most common DNA defects allowed us to detect a change of the shape of the distance distribution. In order to quantify this effect, it is possible to use parameters w (defined before) and r_{mean} and r_{max} which

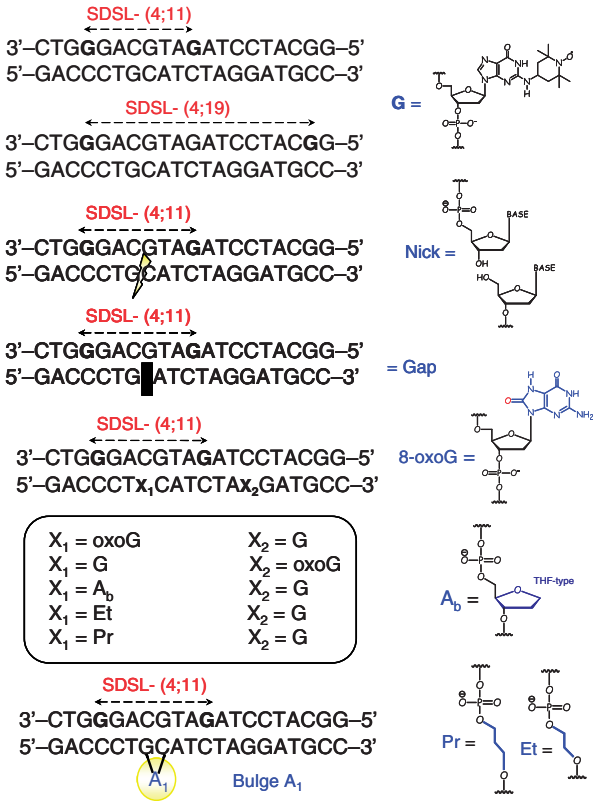

Figure 2. SDSL DNA sequences [4;11] and [4;19]; selected lesions introduced into the DNA duplexes: nick, gap, 8-oxoG, bulge A_1, abasic site and anucleosidic sites.

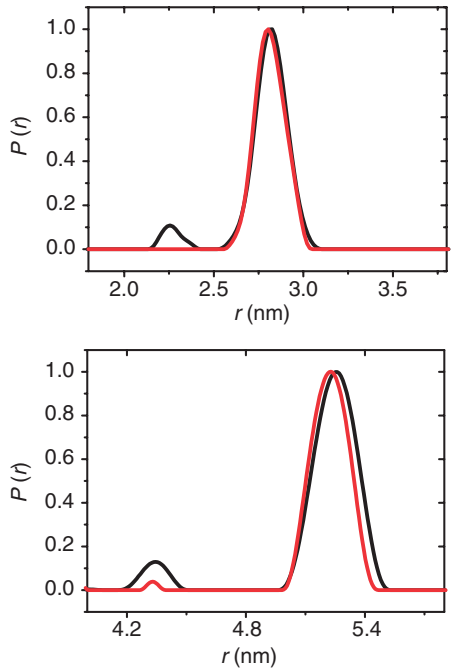

Figure 3. Spin–spin distance distributions obtained by DEER experiments and Tikhonov regularization on undamaged [4;11] (top) and [4;19] duplexes (bottom). Black curves: standard experiments; red curves: orientation averaging experiments with suppression of correlated spin pairs artefact.

are respectively the mean distance computed on the overall distance distribution and the distance corresponding to the maximum of the distribution. In some cases, the main peak is also accompanied by the presence of additional small peaks at longer distance values, probably due to minor conformers of the duplexes. These are excluded from the computation of r_{mean}.

The results summarized in Table 1 allowed us to class DNA lesions into two main groups according to the nature and intensity of the distribution shape modification they induced. The first group only moderately broadens the distance distribution (moderate w increase) and slightly increases the distance r_{max} (Δr very small and positive, where Δr is the difference between the max distance value of the damaged and undamaged duplexes). In particular, the nicked (Figure 4a, blue line), the gap (Figure 4a, purple line), and the bulge (Figure 4a, yellow line) structures did not produce significant distance changes ($|\Delta r| < 0.1$ nm) or modifications of the distribution width ($w \sim 0.22/0.26$). While a slight increase of the width of the distance distribution was observed for the 8-oxoG placed in position 14′ ($w = 0.27$) (Figure 4a, red line), no significant changes were detected for the 8-oxoG placed on position 7′ (Figure 4a, green line) ($w = 0.22$). This is probably due to the relative position of the two paramagnetic centres and of the lesion. In the first case, the damaged base is relatively close and between the spin probes, which is not the case for the other configuration.

Table 1. Parameters of spin–spin distance distributions obtained by orientation averaging DEER experiments and Tikhonov regularization (mean, maximum and width at half height) for undamaged [4;11] duplex and selected lesions

DNA duplex	$r_{[4;11]}$ Mean	$r_{[4;11]}$ Max	w
Undamaged duplex	2.83 ± 0.05	2.81 ± 0.01	0.21 ± 0.02
Nick	2.93 ± 0.03	2.87 ± 0.01	0.22 ± 0.02
Gap	2.95 ± 0.04	2.84 ± 0.01	0.26 ± 0.02
Bulge A_1	2.92 ± 0.03	2.85 ± 0.02	0.23 ± 0.02
8-OxoG (7′)	2.81 ± 0.02	2.81 ± 0.01	0.22 ± 0.02
8-OxoG (14′)	2.81 ± 0.02	2.84 ± 0.01	0.27 ± 0.02
Abasic site (THF)	2.67 ± 0.02	2.46 ± 0.02	0.35 ± 0.02
Ethyl	2.72 ± 0.04	2.65 ± 0.02	0.38 ± 0.04
Propyl	2.70 ± 0.03	2.48 ± 0.02	0.45 ± 0.03

Error values were obtained with a procedure described in the text ('Results' section).

A second group corresponds to DNA lesions which induce both a strong broadening and asymmetry of the distance distribution and a significant distance shortening. The THF-type abasic site (Figure 4a, inset, orange line) and the propyl anucleosidic site (Figure 4a, inset, purple line) exhibit very similar distance distributions with a Δr equal to –0.35 and –0.33, respectively and w equal to 0.35 and 0.45, respectively. It must be noted that due to the pronounced asymmetry with a positive skewness (elongated tail towards the higher distance values) of the distance distribution, the w parameter values in this case can be difficult to compare with data exhibiting a more

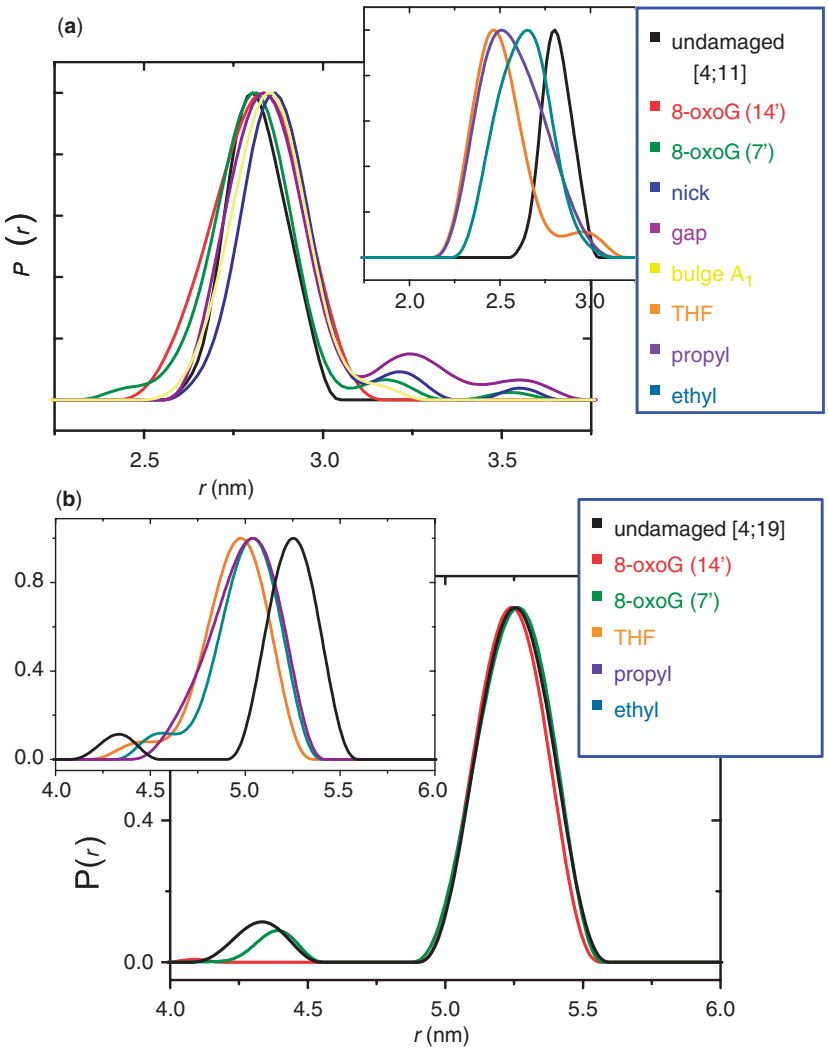

Figure 4. Spin-spin distance distributions obtained by DEER experiments and Tikhonov regularization. (**a**) undamaged [4;11] duplex and selected lesions (*inset*: undamaged duplex, THF, *propyl* and *ethyl* sites). (**b**) undamaged [4;19] duplex and selected lesions (*inset*: undamaged duplex, THF, *propyl* and *ethyl* sites). Distances for the [4;11] duplexes were obtained with an orientation-averaging DEER experiment while distances for the [4;19] duplexes were obtained with a standard experiment (see 'Materials and Methods' section).

symmetrical shape. The ethyl anucleosidic site corresponds to a more moderate Δr value (–0.16) with a significant broadening of distance distribution width ($w = 0.38$) (Figure 4a, inset, cyan line). The shape of this distance distribution is remarkably different from those of the other anucleosidic sites, with only a moderate negative skewness.

Confidence attributed to the results for the [4;11] systems

Reporting results from this type of analysis required a high confidence in r_{max}, r_{mean} and w values obtained for all systems. In particular, one must be sure that the error for these parameters is much lower than the values discussed. In order to obtain estimations for these errors, a two-step approach has been applied.

Primarily, raw data were visually inspected to verify that substantial differences between dipolar evolutions of systems belonging to different groups or to the same group of lesions could be observed without further data treatment. This was quite straightforward as the signal to noise ratio was good, and mutiple oscillations were present (at least two for systems belonging to the second group and three for the systems belonging to the first group).

Important visual differences appear upon comparison of dipolar evolution of systems belonging to the first and second groups of lesions. For instance, the comparison of undamaged, ethyl and propyl systems showed three distinct curves with the last two exhibiting higher frequency (corresponding to smaller distances) than that for the undamaged system (Supplementary Figure S4).

Clear differences were also observed between dipolar evolutions belonging to system of the first group, where variations are much smaller. For instance, superposition of dipolar evolution of the undamaged, the bulge and the nick showed significant differences in oscillation frequency, the fastest oscillation corresponding to the undamaged system and the two slowest corresponding to the

nick and bulge systems (Supplementary Figure S5). This 'visual classification' perfectly corroborates the more elaborate analysis made previously with Tikhonov regularization. Moreover, it is difficult to observe a clear frequency difference between the dipolar evolutions of bulge and nick systems. This is coherent with the quantitative analysis (Table 1).

The direct observation of a slight w increase is much more difficult to observe without appropriate mathematical treatment (fit or Tikhonov regularization). Nevertheless, it is interesting to compare the dipolar evolutions of the undamaged system and of the 8-oxoG on 14′. Visual observation shows that there is a slight decrease in frequency and a more pronounced damping for this system which correspond to a slightly increased distance and a bigger w value (see Table 1 and Supplementary Figure S6).

Secondarily, a more systematic approach was applied. For each lesion at least two different samples were made and studied by pulsed EPR. Raw data from each of these experiments was then submitted to several different, plausible analyses: various background corrections (homogenous, polynomial order), zero-time position, removal of the last points, and addition of extra noise to test solution stability. For each analysis, parameters (r_{max}, r_{mean}, w) were recorded and their dispersion was used to evaluate the error shown in Table 1.

Error values obtained by this procedure were compatible with visual analysis. In particular, they corroborate the fact that it was possible to confidently distinguish two groups of systems and to observe significant differences within the abasic site group. In the first group, as previously determined by visual examination, the difference between the undamaged system and the nick and bulge were easily observable, but these two systems were indistinguishable within error. Strictly speaking, values obtained by this procedure are not 'true' distance errors, since some phenomena, such as spin delocalization along NO nitroxide bond were neglected. Rather, these numbers reflect the sensitivity and reliability of the DEER experiment for the observation of a change in distance between the two spin labels within our set of chemically modified oligonucleotides.

Additional studies on [4;19] DNA duplexes

Selected lesions belonging to the two groups described above were also studied on the [4;19] duplexes in order to confirm the results obtained with the [4;11] duplexes for a wider distance range (Figure 4b and Table 2). In the case of 8-oxoG, no significant differences were detected, with respect to broadening or distance change; it is possible to superimpose the three distance distributions in Figure 4b (green, red and black lines). This result can be explained by the positions of the two lesions with respect to the two spin probes. Distance distribution changes with the same properties (strong w increase, Δr negative and significant) were observed with the THF-type abasic site, the propyl and ethyl anucleosidic sites (Figure 4b, inset), confirming that these three defects induced very pronounced DNA structural changes.

Table 2. Parameters of spin–spin distance distributions obtained by orientation averaging DEER experiments and Tikhonov regularization (mean, maximum and width at half height) for undamaged [4;19] duplex and selected lesions

DNA duplex	$r_{[4;19]}$ Mean	$r_{[4;19]}$ Max	w
Undamaged duplex	5.22 ± 0.04	5.21 ± 0.04	0.33 ± 0.02
8-OxoG (7′)	5.26 ± 0.04	5.23 ± 0.04	0.35 ± 0.03
8-OxoG (14′)	5.25 ± 0.04	5.22 ± 0.04	0.33 ± 0.03
Abasic site (THF)	4.95 ± 0.05	4.97 ± 0.03	0.42 ± 0.03
Ethyl	5.04 ± 0.05	5.02 ± 0.03	0.39 ± 0.05
Propyl	4.89 ± 0.05	5.02 ± 0.03	0.44 ± 0.05

Error values were obtained with a procedure described in the text ('Results' section).

The same procedures as discussed above (visual analysis and the more systematic approach) were used to evaluate errors in the [4;19] systems (Supplementary Figures S7 and S8 and Table 2). Again, it was possible to clearly distinguish between the two groups of lesions. But qualitative and quantitative error analysis shows that the uncertainty is much higher than found with the [4;11] systems. In particular, it is impossible to distinguish between the undamaged and the two 8-oxoG derivatives. This could be attributed in part to a 'blurring' effect due to a much more demanding DEER analysis for longer distance ranges (7). This is also probably why in the [4;19] experiment, the three anucleosidic sites produce very analogous distance distributions while in the [4;11] experiment, the ethyl anucleosidic site was clearly distinguishable.

Comparison with molecular dynamics

In order to provide a more comprehensive description and to confirm the effects induced by lesions, a molecular dynamics study was carried out on at least one [4;11] lesion for each of the groups defined above, namely the undamaged structure, the nick, the gap, the 8-oxoG (14′) and the THF abasic site. A complete description of the ^{TEMPO}G–C base pair properties, taking into account the internal flexibility of the ^{TEMPO}G-C base pair and providing details on the combination of the base pairs, as well as model built before the minimization of the overall DNA structures, are described elsewhere.

There is very good agreement between experimental and MD interspin distances, with a sligh systematic overestimation in the calculated data of the order of ~0.16 nm for the duplexes depicted in Table 1. Concerning the Δr values, the agreement between experimental and theoretical data is excellent.

It is possible to reproduce the trend observed in DEER experiments for the 8-oxoG, gap and nick structure: a slight increase of distance and of width [Table 3 and Figure 5, nick (blue line), 8-oxoG (red line), gap (green line)]. For the duplexes containing an 8-oxoG base paired with a cytosine, DEER distances and MD simulations demonstrate that this modified base pair does not perturb the *B*-DNA helix. For the nick and gap duplexes, distances measured experimentally or extracted from MD simulations show that structural perturbations induced

Table 3. Parameters of global normalized fitted gaussian distributions of the NO–NO distance obtained by MD studies for the undamaged [4;11] duplex and selected lesions

DNA duplex	$r^{NONO}_{(MD)}$	$\Delta r_{(MD)}$	Δr_{DEER}
Undamaged [4;11]	2.97		
Nick	3.06	+0.09	+0.06
Gap	3.11	+0.14	+0.03
8-OxoG (7′)	2.98	+0.01	+0.01
Abasic site (THFext-Cext)	2.70	–0.27	–0.35
Abasic site (THFext-Cint)	2.90	–0.07	n.d.

n.d.: not determined. Comparison between Δr from DEER experiments and MD are also given for these systems.

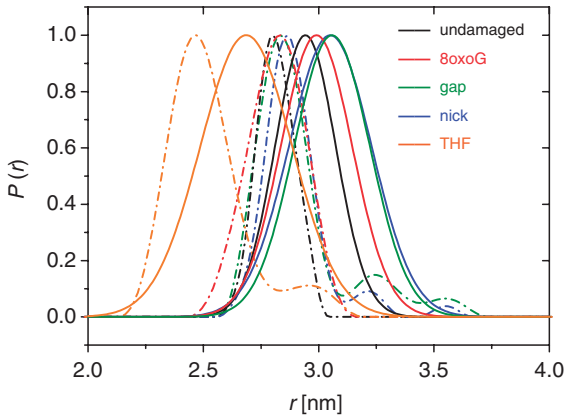

Figure 5. Global normalized Gaussian-fit distributions of the NO–NO distance obtained by MD studies (solid line) and distance distributions from DEER experiment (dashed line, see Figure 4) for the undamaged (black line), nick (blue line), 8-oxoG (red line), gap (green line), THF with both THF residue and extrahelical cytosine (orange line) [4;11] systems.

by this common lesions are subtle. The main difference detected between the two studies (MD versus DEER) concerns the w parameter. Higher values are observed for both damaged and undamaged duplexes in MD, running from $w = 0.31$ nm (undamaged [4;11] duplex) up to $w = 0.47$ nm for the for the [4;11] duplex containing the THF abasic site compared to those measured by DEER analysis ($w = 0.21$ nm and $w = 0.35$ nm, respectively). This discrepancy is probably due to the different temperature set up: for the DEER experiment the systems were analysed in frozen solution (60–70 K) while the computational studies were carried out at room temperature. Thus, strictly speaking, w parameters provided by DEER experiments and those calculated by molecular dynamics are not related to the same phenomena. The former $w_{(DEER)}$ describes the set of different conformations trapped during the freezing processes while the latter $w_{(MD)}$ comes from the simulated flexibility of one molecule in solution.

For the abasic (THF) site, a first model where both the THF and the cytosine are placed inside the helix was built as a starting conformation (Figure 6a). During this simulation, the THF abasic site moves spontaneously from an intrahelical position to an extrahelical position and remains outside during the remainder of calculations. The phosphate backbone forms a right-handed loop (38) leading the THF residue to move into the minor groove, leaving it completely exposed to the solvent. On the contrary, the cytosine facing the THF site remains intrahelical during the entire simulation (Figure 6b). The Δr obtained for this conformation ($\Delta r = –0.07$, Table 3) does not reproduce the EPR data very closely ($\Delta r = –0.35$). The simulation with a model where the cytosine is intrahelical and the THF is extrahelical leads to a similar result except that the flip out of THF is faster and the distance obtained is closer to the experimental one ($\Delta r = –0.18$, data not shown). Taking into account these results and a previous study on abasic sites (39) a model where *both* THF and cytosine are extra-helical has been built (Figure 6c). This structure remains stable during the whole MD calculation and the Δr obtained is higher ($\Delta r = –0.27$ nm, Table 3 and Figure 5, solid orange curve) and close to the experimental one ($\Delta r = –0.35$). The strong asymmetry with positive skewness observed in the shape of the experimental distance distribution for the abasic (THF) site can be related to the coexistence in solution of the two conformations described above. The probable presence of intermediate conformations precludes the observation of individual peaks for in/out and out/out systems.

DISCUSSION

Synthetic oligonucleotides containing selective lesions at defined sites are powerful tools to study the biological features of DNA alterations, in terms of repair, replication and mutagenesis (40–42). Such modified nucleic acid probes may also be used to determine the structural modifications induced by selective lesions. High resolution NMR spectroscopy has been shown to be a method of choice and a large set of studies have been performed on synthetic lesion-containing DNA fragments and reported in the literature [see (11) for a recent review]. To overcome some drawbacks inherent in the latter spectroscopie approach (see 'Introduction' section), we have applied SDSL combined with pulsed EPR techniques (DEER) for the first time to the structural analyses of several damaged DNA fragments.

Due to a moderate interspin distance of around 3 nm and a very rigid structure, this strategy allowed us to optimally measure the distance distribution shape for the [4;11] system. The rigidity of the system may explain why it was possible to measure a distance up to 5.3 nm for the [4;19] duplexes with a high precision. This represents a significant improvement of the SDSL approach, compared with the labelled systems described in the literature (32–34). The combined approach: pulsed EPR and spin labelling allowed the study of 20 bp oligonucleotides. This is in contrast to the most common dodecamer described in literature. This may represent a remarkable tool for the study of long-range lesion-amplification in the overall structure of the bio-system. Due to DEER limitations on long distance determinations (~6.0 nm), measurements on [4;19] systems are less accurate and simply confirm the classification of DNA lesions studied in both groups.

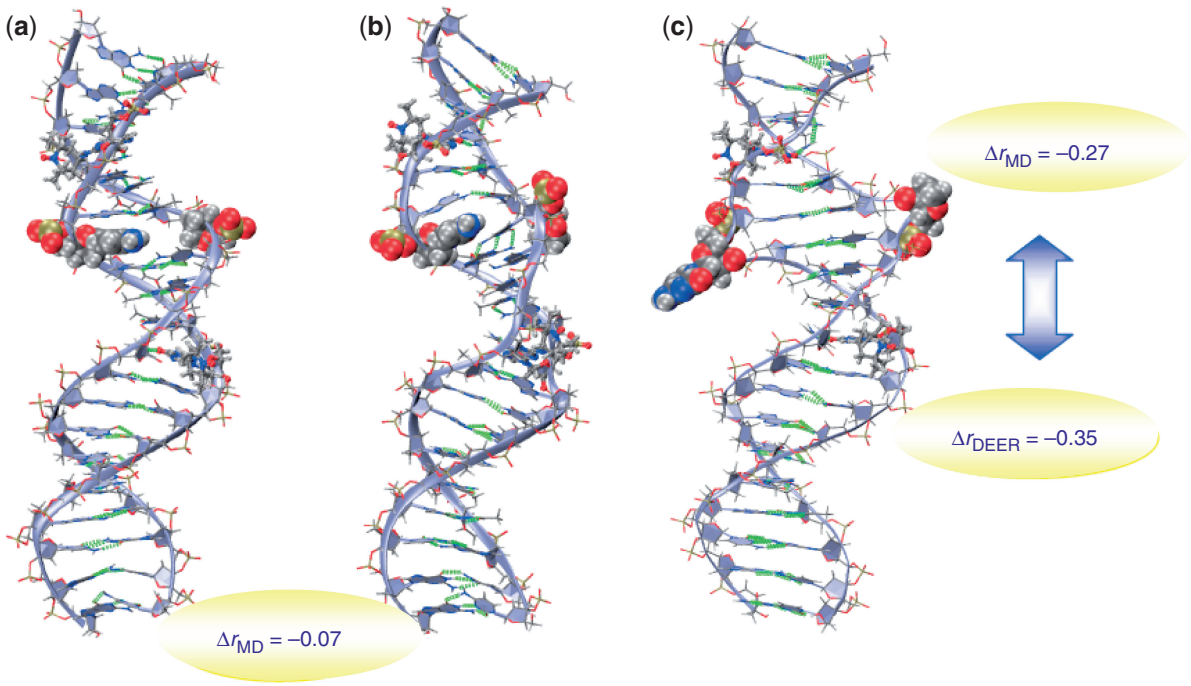

Figure 6. Snapshots of structures used for the [4;11] THF systems and their opposing C base residue: (**a**) both C and THF intrahelical; (**b**) THF extrahelical and C intrahelical; (**c**) both C and THF extrahelical.

The overview described in this work allowed us to classify two different kinds of induced DNA structural changes: group (i) where only the flexibility of the system is mildly affected producing a somewhat broader distance distribution than the undamaged duplex, and the distance is slightly increased (nick, gap, bulge and 8-oxoG lesions); group (ii) where the distance distribution is significantly shortened with an asymmetric and very large distance distribution (abasic sites analogues).

According to previous studies, the 8-oxoG lesion does not profoundly perturb the DNA structure. For instance, according to NMR studies (43), for a self-complementary dodecamer containing two 8-oxoGC base pairs, an *anti* conformation forming regular Watson–Crick (WC) alignments has been observed. Similarly, the H_7 proton of 8-oxoG also resonates at typical chemical shift (10 ppm) and no NOE interactions are observed, a fact which is consistent with major groove localization of the damaged base (44). This negligible perturbation of the overall system has been confirmed by the DEER measurement with a very small Δr and a moderate broadening. This broadening can confidently be attributed to real conformational variability and is not a DEER data analysis artefact. Indeed the shape/broadening of the distance distribution and the corresponding w value have been found to be reproducible and robust with respect to signal to noise ratio, sample concentration, type of DEER experiment (1D or 2D, see 'Materials and Methods' section) and data analysis parameters (baseline correction, Tikhonov regularization parameters). This broadening is pronounced ($w = 0.27$) when the damaged base is placed at a comparable distance between the spin labels while it is very small ($w = 0.22$) when the damaged base is closer to one of the probes and far from the second one. This result seems to indicate that the broadening is not due to a (independent) destabilization of the spin probe position induced by the 8-oxoG, but rather is due to increased flexibility of the whole system. This broadening effect is not clearly visible for the [4;19] duplexes. But in this case, as discussed above, the higher distance range precludes a very precise analysis of broadening. To our knowledge, this increased flexibility has not been observed with other methods or MD studies which even describe a slight decrease in flexibility for this system (unpublished results). The origin of this discrepancy is unknown but it must be noted that DEER experiments were performed in frozen solution while NMR and MD studies were performed in aqueous solution. It has been demonstrated that during the freezing process, spin label movements can occur (45).

In this study, the smallest perturbations are found to be produced by the nick, gap and bulge structures. This result is in agreement with the previous data reported in the literature for the nick. In particular, early electrophoretic studies of nicked duplexes have shown that formation of a strand break does not cause a significant increase of DNA flexibility, implying that the DNA around the lesion essentially retains its ordered structure (46). Subsequent NMR studies have clearly confirmed this suggestion (47). According to the literature, perturbations induced by a gap structure are more important (48). Despite differences in lesion-site stability, the NMR characterization of gap-containing duplexes indicates the presence of a classical *B*-type conformation with the orphan adenine or guanine residues stacked in the helix (48).

Results from MD and DEER show unambiguously that both the THF abasic site and its opposing cytosine base are extrahelical. Several studies have established that oligonucleotides containing abasic sites opposite purine residues conserve a *B*-DNA geometry in which the base opposite the lesion stacks inside the helix (49). On the contrary, duplexes containing abasic sites opposite pyrimidine residues display additional forms where the abasic sugar and sometimes the opposite pyrimidine are extrahelical (50). Thus, even if it was previously suggested that the flip-out of an abasic site may be favoured when it is flanked by two purines, due to the important gain in stacking energy compared to an abasic site flanked by two pyrimidines (51), our study demonstrates that when two pyrimidines flank a THF residue, the abasic site is also flipped out. This result cannot be generalized since conformational changes in DNA have been shown to be sequence-context dependent (52–55).

While in frozen solution the major conformation is *out-out*, the asymmetric distance distribution with an elongated tail toward longer distances may be explained by the presence of minor conformations (see Results: comparison MD-DEER). This can be attributed to the intrinsic flexibility of the studied duplex. For the propyl abasic site, a similar shape has been obtained by DEER indicative of a main conformation with an extrahelical position for the propyl chain and other minor conformations in which the alkyl chain is intrahelical. The extrahelical conformation is probably involved in the recognition of damage by some DNA *N*-glycosylase proteins such as Fapy DNA glycosylase from *E. coli* (*ec*Fpg) as observed by X-ray crystallography (56). It is interesting to note that the above-mentioned conformations have been observed (in our work) in the absence of protein. As reported in literature, both AP analogues are flipped out of the DNA helix by *ec*Fpg at the lesion site and a local decrease of the phosphate-phosphate distance is observed (56). In all the described structures the AP site analogue is not directly in contact with Fpg residues (56) confirming that the flip-out of the DNA damage is probably a prerequisite for the enzymatic recognition process.

On the contrary, the distance distribution for the ethyl abasic site analogue is clearly different with an elongated tail towards shorter distances. In the absence of further data in the literature, it is difficult to propose a precise global structure for this system but a different conformation can reasonably be deduced with respect to the two other abasic site analogues mentioned above (57). It is interesting to underline that this last analogue is only weakly recognized by the Fpg repair protein while the first two residues (THF and propyl) exhibit a strong affinity for this protein. Thus, distance distributions combined with molecular dynamics studies might also be a promising tool for analysing the interactions of DNA–protein complexes containing abasic sites analogues. These analogues could provide further details about the recognition (and repair) mechanism of DNA lesions which is still not completely rationalized at this date.

CONCLUSIONS

The SDSL approach, combined with pulsed EPR analyses and molecular dynamics simulations seems to provide a complementary and powerful tool for DNA damage analyses with respect to the most common analytical techniques (NMR, CD, X-ray crystallography, FRET). The possibility to prepare and analyse two different double SDSL systems may provide further information related to the relative nitroxide position and/or to their position with respect to the selected lesion. Furthermore, the influence of the derivatization pattern on the distance distribution may be readily related to their *width*. Both EPR experimental data and MD simulations converge to the same distance changes, demonstrating that the combination of these two methods is adapted to the study of the influence of a specific lesion on DNA structure. The promising results described in this work suggest several future applications such as in DNA–protein interactions studies, in order to provide specific insights into the repair mechanism of selected lesions. Conformational changes induced in DNA structures by covalent and non-covalent interactions with small molecules (intercalating agents, peptides, metal complexes) should be also addressed.

SUPPLEMENTARY DATA

Supplementary Data are available at NAR Online.

ACKNOWLEDGEMENTS

The authors thank G. Desfonds for technical help on EPR spectrometers and Maighread Gallagher for reading the manuscript.

FUNDING

Agence Nationale de la Recherche [ANR-05-BLAN-0064-01]. Funding for open access charge: CEA-Grenoble.

Conflict of interest statement. None declared.

REFERENCES

1. Friedberg,E.C. (2003) DNA damage and repair. *Nature*, **421**, 436–440.
2. Lindahl,T. (1993) Instability and decay of the primary structure of DNA. *Nature*, **362**, 709–715.
3. Cadet,J., Bellon,S., Douki,T., Frelon,S., Gasparutto,D., Muller,E., Pouget,J.P., Ravanat,J.-L., Romieu,A. and Sauvaigo,S. (2004) Radiation-induced DNA damage: formation, measurement, and biochemical features. *J. Environ. Pathol. Toxicol. Oncol.*, **23**, 33–43.
4. Schärer,O.D. (2003) Chemistry and Biology of DNA Repair. *Angew. Chem. Int. Ed.*, **42**, 2946–2974.
5. Bjelland,S. and Seeberg,E. (2003) Mutagenicity, toxicity and repair of DNA base damage induced by oxidation. *Mutat. Res.*, **531**, 37–80.
6. Friedberg,E.C., Walker,G.C. and Siede,W. (2006) (eds), *DNA Repair and Mutagenesis*, 2nd edn. American Society for Microbiology Press, Washington, DC.
7. Jeschke,G. and Polyhach,Y. (2007) Distance measurements on spin-labelled biomacromolecules by pulsed electron paramagnetic resonance. *Phys. Chem. Chem. Phys.*, **9**, 1895–1910.

8. Schiemann,O., Piton,N., Plackmeyer,J., Bode,E.B., Prisner,T.E. and Engels,J.W. (2007) Spin labeling of oligonucleotides with the nitroxide TPA and use of PELDOR, a pulse EPR method, to measure intramolecular distances. *Nat. Protocols*, **2**, 904–921.
9. Schiemann,O. and Prisner,T.F. (2007) Long-range distance determination in biomacromolecules by EPR spectroscopy. *Quart. Rev. Biophys.*, **40**, 1–53.
10. Klug,C.S. and Feix,J.B. (2008) Methods and applications of site-directed spin labeling EPR spectroscopy. *Methods Cell Biol.*, **84**, 617–658.
11. Lukin,M. and De los Santos,C. (2006) NMR structures of damaged DNA. *Chem. Rev.*, **106**, 607–686.
12. Norman,D.G., Grainger,R.J., Uhrin,D. and Lilley,D.M.J. (2000) Location of Cyanine-3 on double-stranded DNA: importance for fluorescence resonance energy transfer studies. *Biochemistry*, **39**, 6317–6324.
13. Majumdar,Z.K., Hickerson,R., Noller,H.F. and Clegg,R.M. (2005) Measurements of internal distance changes of the 30 S ribosome using FRET with multiple donor–acceptor pairs: quantitative spectroscopic methods. *J. Mol. Biol.*, **351**, 1123–1145.
14. Hillisch,A., Lorenz,M. and Diekmann,S. (2001) Recent advances in FRET: distance determination in protein–DNA complexes *Curr. Opin. Struct. Biol.*, **11**, 201–207.
15. Jose,D. and Porschke,D. (2004) Dynamics of the B–A transition of DNA double helices. *Nucleic Acids Res.*, **32**, 2251–2258.
16. Nejedlý,K., Chládková,J., Vorlícková,M., Hrabcová,I. and Kypr,J. (2005) Mapping the B-A conformational transition along plasmid DNA. *Nucleic Acids Res.*, **33**, e5.
17. Ivanov,V.I., Minchenkova,L.E., Burckhardt,G., Birch-Hirschfeld,E., Fritzsche,H. and Zimmer,C. (1996) The detection of B-form/A-form junction in a deoxyribonucleotide duplex. *Biophys. J.*, **71**, 3344–3349.
18. Hara,H., Tenno,T. and Shirakawa,M. (2007) Distance determination in human ubiquitin by pulsed double electron-electron resonance and double quantum coherence ESR methods. *J. Magn. Reson.*, **184**, 78–84.
19. Borbat,P.P. and Freed,J.H. (1999) Multiple-quantum ESR and distance measurements. *Chem. Phys. Lett*, **313**, 145–154.
20. Borbat,P.P., Mchaourab,H.S. and Freed,J.H. (2002) Protein structure determination using long-distance constraints from double-quantum coherence ESR: study of T4 lysozyme. *J. Am. Chem. Soc.*, **124**, 5304–5314.
21. Milov,A.D., Tsvetkov, Yu,D., Formaggio,F., Crisma,M., Toniolo,C. and Raap,J. (2000) Self-assembling properties of membrane-modifying peptides studied by PELDOR and CW-ESR spectroscopies. *J. Am. Chem. Soc.*, **122**, 3843–3848.
22. Hilger,D., Polyhach,Y., Padan,E., Jung,H. and Jeschke,G. (2007) High-resolution structure of a Na^+/H^+ antiporter dimmer obtained by pulse electron paramagnetic resonance distance measurements. *Biophys. J.*, **93**, 3675–3683.
23. Schiemann,O., Weber,A., Edwards,T.E., Prisner,T.F. and Sigurdsson,S.T. (2003) Nanometer distance measurements on RNA using PELDOR. *J. Am. Chem. Soc.*, **125**, 3434–3435.
24. Schiemann,O., Piton,N., Mu,Y., Stock,G., Engels,J.W. and Prisner,T.F. (2004) A PELDOR-based nanometer distance ruler for oligonucleotides. *J. Am. Chem. Soc.*, **126**, 5722–5729.
25. Borbat,P.P., Davis,J.H., Butcher,S.E. and Freed,J.H. (2004) Measurement of large distances in biomolecules using double-quantum filtered refocused electron spin-echoes. *J. Am. Chem. Soc.*, **126**, 7746–7747.
26. Sicoli,G., Mathis,G., Delalande,O., Boulard,Y., Gasparutto,D. and Gambarelli,S. (2008) Double electron-electron resonance (DEER): a convenient method to probe DNA conformational changes. *Angew. Chem. Int. Ed.*, **47**, 735–737.
27. Gasparutto,D., Saint Pierre,C., Jaquinod,M., Favier,A. and Cadet,J. (2003) MALDI-TOF MS as a powerful tool to study enzymatic processing of DNA lesions inserted into oligonucleotides. *Nucleosides, Nucleotides Nucleic Acids*, **22**, 1583–1586.
28. Okamoto,A., Inasaki,T. and Saito,I. (2004) Nitroxide-labeled guanine as an ESR spin probe for structural study of DNA. *Bioorg. Med. Chem. Lett.*, **14**, 3415–3418.
29. Bourdat,A.-G., Gasparutto,D. and Cadet,J. (1999) Synthesis and enzymatic processing of oligonucleotides containing tandem base damage. *Nucleic Acids Res.*, **27**, 1015–1024.
30. Romieu,G., Gasparutto,D., Molko,D. and Cadet,J. (1997) A convenient synthesis of 5-hydroxy-2′-deoxycytidine phosphoramidite and its incorporation into oligonucleotides. *Tetrahedron Lett.*, **43**, 7531–7534.
31. Jeschke,G., Chechik,V., Ionita,P., Godt,A., Zimmermann,H., Banham,J., Timmel,C.R., Hilger,D. and Jung,H. (2006) DeerAnalysis 2006 – a comprehensive software package for analyzing pulsed ELDOR data. *Appl. Magn. Reson.*, **30**, 473–498.
32. Cai,Q., Kusnetzow,A.K., Hubbell,W.L., Haworth,I.S., Gacho,G.P.C., Van Eps,N., Hideg,K., Chambers,E.J. and Qin,P.Z. (2006) Site-directed spin labeling measurements of nanometer distances in nucleic acids using a sequence-independent nitroxide probe. *Nucleic Acids Res.*, **34**, 4722–4730.
33. Ward,R., Keeble,D.J., El-Mkami,H. and Norman,D.G. (2007) Distance determination in heterogeneous DNA model systems by pulsed EPR. *ChemBioChem*, **8**, 1957–1964.
34. Piton,N., Mu,Y., Stock,G., Prisner,T.F., Schiemann,O. and Engels,J.W. (2007) Base-specific spin-labelling of RNA for structure determination. *Nucleic Acids Res.*, **35**, 3128–3143.
35. Larsen,R.G. and Singel,D.J. (1993) Double electron-electron resonance spin-echo modulation: spectroscopic measurement of electron spin pair separations in orientationally disordered solids. *J. Chem. Phys.*, **98**, 5134–5146.
36. Margraf,A., Bode,B.E., Marko,A., Schiemann,O. and Prisner,T.F. (2007) Conformational flexibility of nitroxide biradicals determined by X-band PELDOR expriments. *Mol. Phys.*, **105**, 2153–2160.
37. Godt,A., Schulte,M., Zimmermann,H. and Jeschke,G. (2006) How flexible are poly(*para*-phenyleneethynylene)s? *Angew Chem Int Ed.*, **45**, 7560–756.
38. Maufrais,C., Fazakerley,G.V., Cadet,J. and Boulard,Y. (2003) Structural study of DNA duplex containing an N-(2-deoxy-beta-D-erythro-pentofuranosyl) formamide frameshift by NMR and restrained molecular dynamics. *Nucleic Acids Res*, **31**, 5930–5940.
39. Cuniasse,P., Fazakerley,G.V., Guschlbauer,W., Kaplan,B.E. and Sowers,L.C. (1990) The abasic site as a challenge to DNA polymerase. A nuclear magnetic resonance study of G, C and T opposite a model abasic site. *J. Mol. Biol.*, **213**, 303–314.
40. Wang,D., Kreutzer,D.A. and Essigmann,J.M. (1998) Mutagenicity and repair of oxidative DNA damage: insights from studies using defined lesions. *Mutat. Res.*, **400**, 99–115.
41. Butenandt,J., Burgdorf,L.T. and Carell,T. (1999) Synthesis of DNA lesions and DNA-lesion-containing oligonucleotides for DNA-repair studies. *Synthesis*, **7**, 1085–1105.
42. Gasparutto,D., Bourdat,A.G., D'Ham,D., Duarte,V., Romieu,A. and Cadet,J. (2000) Repair and replication of oxidized DNA bases using modified oligodeoxyribonucleotides. *Biochimie*, **82**, 19–24.
43. Oda,Y., Uesugi,S., Ikehara,M., Nishimura,S., Kawase,Y., Ishikawa,H., Inoue,H. and Ohtsuka,E. (1991) NMR studies of a DNA containing 8-hydroxydeoxyguanosine. *Nucleic Acids Res.*, **19**, 1407–1412.
44. Gannett,P.M. and Sura,T.P. (1993) Base pairing of 8-oxoguanosine and 8-oxo-2′-deoxyguanosine with 2′-deoxyadenosine, 2′-deoxycytosine, 2′-deoxyguanosine, and thymidine. *Chem. Res. Toxicol.*, **6**, 690–700.
45. Banham,J.E., Jeschke,G. and Timmel,C.R. (2007) Evidence from EPR that nitroxide spin labels attached to human hemoglobin alter their conformation upon freezing. *Mol. Phys.*, **105**, 2041–2047.
46. Mills,J.B., Cooper,J.P. and Hagerman,P.J. (1994) Electrophoretic evidence that single-stranded regions of 1 or more nucleotides dramatically increase the flexibility of DNA. *Biochemistry*, **33**, 1797–1803.
47. Singh,S., Patel,P. and Hosur,R.V. (1997) Structural polymorphism and dynamism in the DNA segment GATCTTCCCCCGGAA: NMR investigations of hairpin, dumbbell, nicked duplex, parallel strands, and i-motif. *Biochemistry*, **36**, 13214–13222.
48. Roll,C., Ketterlé,C., Faibis,V., Fazakerley,G.V. and Boulard,Y. (1998) Conformations of nicked and gapped DNA structures by NMR and molecular dynamic simulations in water. *Biochemistry*, **37**, 4059–4070.
49. Takeshita,M., Chang,C.-N., Johnson,F., Will,S. and Grollman,A.P. (1987) Oligodeoxynucleotides containing synthetic abasic sites. *J. Biol. Chem.*, **262**, 10171–10179.
50. Pompizi,I., Häberli,A. and Leumann,C.J. (2000) Oligodeoxynucleotides containing conformationally constrained

abasic sites: a UV and fluorescence spectroscopic investigation on duplex stability and strcuture. *Nucleic Acids Res.*, **28**, 2702–2708.
51. Hoehn,S.T., Turner,C.J. and Stubbe,J. (2001) Solution structure of an oligonucleotide containing an abasic site: evidence for an unusual deoxyribose conformation. *Nucleic Acids Res.*, **29**, 3413–3423.
52. O'Neil,L.L. and Wiest,O. (2008) Sequence dependence in base flipping: experimental and computational studies. *Org Biomol. Chem.*, **6**, 485–492.
53. Ayadi,L., Coulombeau,C. and Lavery,R. (1999) Abasic sites in duplex DNA: molecular modelling of sequence-dependent effects on conformation. *Biophys. J.*, **77**, 3218–3226.
54. Krueger,A., Protonazova,E. and Frank-Kamenetskii,M.D. (2006) Sequence-dependent base pair opening in DNA double helix. *Biophys. J.*, **90**, 3091–3099.
55. Chen,J., Dupradeau,F.-Y., Case,D.A., Turner,C.J. and Stubbe,J. (2008) DNA oligonucleotides with A, T, G or C opposite an abasic site: structure and dynamics. *Nucleic Acids Res.*, **36**, 253–262.
56. Pereira de Jésus,K., Serre,L., Zelwer,C. and Castaing,B. (2005) Structural insights into abasic site for Fpg specific binding and catalysis: comparative high-resolution crystallographic studies of Fpg bound to various model of abasic site analogues-containing DNA. *Nucleic Acids Res.*, **33**, 5936–5944.
57. Vesnaver,G., Chang,C.-N., Eisenberg,M., Grollman,A.P. and Breslauer,K.J. (1989) Influence of abasic and anucleosidic sites on the stability, conformation and melting behaviour of a DNA duplex: correlations of thermodynamic and structural data. *Proc. Natl Acad. Sci. USA*, **86**, 3614–3618.